Journal of Geochemical Exploration 197 (2019) 48–59

Contents lists available at ScienceDirect

Journal of Geochemical Exploration

journal homepage: www.elsevier.com/locate/gexplo

Geo-statistical and multivariate analyses of potentially toxic elements' distribution in the soil of Hainan Island (China): A comparison between the topsoil and subsoil at a regional scale

An-Ting Wang[a], Qi Wang[a], Jun Li[a], Guo-Li Yuan[a,b,*], Stefano Albanese[c], Attila Petrik[c]

[a] School of the Earth Sciences and Resources, China University of Geosciences, Beijing 100083, China
[b] State Key Laboratory of Biogeology and Environmental Geology, Beijing 100083, China
[c] Dipartimento di Science della Terra, dell'Ambiente e delle Risorse, University of Naples Federico II, Napoli 80126, Italy

ARTICLE INFO

Keywords:
Potentially toxic elements
Topsoil
Subsoil
Geo-statistical and multivariate analyses
Impact factors

ABSTRACT

Geo-statistical and multivariate analyses are effective methods to determine the source and influence factors of potentially toxic elements (PTEs) in the soil. Hainan Island, belonging to tropical marine monsoon climate, is a typically individual island with slight industrial activities. In order to study the impact factors on PTEs distribution in the soil at a regional scale, such as impact of lithology, pedogenesis and anthropogenic activities, Hainan Island is an optimal place. For comparison, the topsoil and the corresponding subsoil were sampled and eight PTEs were analyzed respectively. The concentrations of PTEs were counted, such as minimum, maximum, median and mean values. Based on it, the background values and concentration enrichment factors of PTEs were also calculated or illustrated. Exception to Cd and Hg, the concentration of other PTEs in the topsoil were lower than those in the subsoil for all lithological areas since the strong leaching under special climate. By using geo-statistical and multivariate analyses, such as Pearson correlation analysis, principal component analysis, variography and robust biplot analyses, the dominant impact factors are determined for PTEs both in the topsoil and subsoil. Thus, the spatial distribution of PTEs is well explained at a regional scale. Generally, PTEs in the soil represent the components of soil parent materials associated with lithological rocks. Nevertheless, Co, Cr, Cu and Sc elements were dominantly inherited from soil parent materials while Cd, Hg and Pb were greatly superposed by exogenous inputs. On the other hand, elements of As and Zn might be greatly influenced by pedogenesis and weathering process. So, geo-statistical and multivariate analyses are effective methods to discuss the sources or impact factors for PTEs in the soil, and also the comparison between the topsoil and the subsoil provides an opportunity to illuminate the main impact factors on PTEs at a regional scale, including parent materials, weathering process and anthropogenic inputs.

1. Introduction

Soil contaminations with potential toxic elements (PTEs) attract a worldwide environmental attention mainly because these elements can transfer to the hydrosphere, biosphere and food chain, finally posing a hazard to human health (Fu et al., 2011; Nannoni et al., 2011; Lu et al., 2012). The soil can be considered as the ultimate product of different combined processes including the weathering of parent materials, the accumulation, the decomposition, the humification of organic matter and the synergistic action of some influencing factors such as climate, topography, organisms (soil microbiology, mesofauna and biology), time and further state variables (Salminen and Gregorauskiene, 2000; Palumbo et al., 2000; Adot et al., 2006; Qishlaqi et al., 2009; Bini et al., 2011). Although the evolution rate of this nature is very low, the original mineral components and PTEs in soil parent materials mainly come from native rocks. To a large extent, the soil parent materials mainly determine the properties of soils (Rodríguez et al., 2006; Bini et al., 2011; Lv et al., 2013). Nevertheless, PTEs in soils can be influenced at different extent by biogeochemical process or anthropogenic sources (Meklit et al., 2009; Lv et al., 2013). Sometimes, soils in a place far away from human activities might enrich PTEs due to the transport of anthropogenic sources (Acosta, 2011). Thus, the spatial distribution of PTEs in soils may be affected by both parent materials and anthropogenic input (Bini et al., 2011; Hanesch et al., 2001; Meklit et al., 2009). For this reason, it is important to look for the relationships of PTEs between in the soils and in its parent material. Then, the influence

* Corresponding author at: School of Earth Sciences and Resources, China University of Geosciences, Beijing 100083, China.
E-mail address: yuangl@cugb.edu.cn (G.-L. Yuan).

https://doi.org/10.1016/j.gexplo.2018.11.008
Received 14 July 2018; Received in revised form 24 October 2018; Accepted 17 November 2018
Available online 24 November 2018
0375-6742/

degree of human activities on PTEs can be determined.

The concentration of PTEs in the topsoil include the naturally geogenic background concentrations and the input of anthropogenic contribution (Facchinelli et al., 2001; Salminen and Gregorauskiene, 2000; Frattini et al., 2006; Albanese et al., 2007). Traditionally, background values of PTEs in the subsoil can act as background for evaluating the pollution extent of PTEs in certain areas (Ansari et al., 2000; Rognerud et al., 2000). However, due to the long-term weathering and leaching, the PTEs in topsoil are easily depleted compared to those in the subsoil. More importantly, such a process is different from the different soil parent materials. So far, little data about water-leaching risk of PTEs in different parent materials have been reported. Instead of background value, the concentration of PTEs in the subsoil can act as a reference standard to evaluate the enrichment/loss extent of PTEs, which is tentatively named as Concentration Enrichment Factor (CEF) (Fergusson, 1990). Although such a method has been less reported, CEF may be more exactly evaluate the enrichment/loss extent of PTEs in topsoil, especially for warm and rainy areas. To some extent, the concentration of PTEs in subsoil is closely associated with the soil parent materials.

Geo-statistical and Multivariate analyses (GSMA) are useful tools for quantifying the spatial characteristics and determining the relationship of PTEs and their possible sources (Yuan et al., 2013, 2014). By GSMA, a whole regionalized variable could be split into different components related to different scales of spatial correlation according to the parent materials (Alary and Demougeot-Renard, 2010). The analyses of PTEs' distribution in soil at different observation scales can bring different insights (Saby et al., 2009).

Hainan Island, the second largest island in southern China, is one province of China. The soil in Hainan Island was little polluted by modern industrial since the predominant activities are tourism and green agriculture, which is different from other places in China (Fu et al., 2011; Gong et al., 2014). Nevertheless, the recently increasing human activities, such as travel, also affect the level of PTEs in the soil of Hainan province (Quinton and Catt, 2007; Wang et al., 2013; Hao et al., 2009; Li et al., 2009; Gong et al., 2014). On the other hand, the warm and rainy climate In Hainan Island may accelerate the leaching of PTEs from the topsoil (Gong et al., 2014). As introduced above, analysis of PTEs contents in the subsoil is very important for studying them in the topsoil. So, it is significant to compare and assess the PTEs in the topsoil and the subsoil with different parent materials at regional scale.

The objectives of this study are: (1) to systematically map their spatial distributions and patterns of PTEs in topsoils and subsoils; (2) to identify their background values in subsoils and baseline values in topsoils; (3) to evaluate CEF and possible hot zones of PTEs in each type of geological region of Hainan Island; (4) to determine their controlling sources and the main influence factors on PTEs distribution in soils.

2. Materials and methods

2.1. Study area and sampling

The study area of Hainan Island (108°37′–111°03′E, 18°10′–20°10′N) is located in the southernmost China, occupies 33,920 km^2 of land area (Fig. 1) and separated from the mainland by a narrow strait. The climate is a typical tropical marine monsoon with an annual temperature of 23–26 °C and average annual precipitation of 1500–2500 mm. The major soil type is latosol (pH, 5.0) with a complex terrain of plains and hills staggered (Gong et al., 2014). In the island (Fig. 1), granite is the most extensive parent rock, accounting for nearly 50% of outcrops of the total parent rocks; whereas basalt, mainly located in the northern sector of the island, accounts for 13.6%; mesozoic sedimentary rocks are mostly in the central part and metamorphic rocks are little represented. Around the island, the coastline is mostly characterized by quaternary sediments, generally, derived from the weathering of the geological material outcropping in the island inner part.

During April 2004, 8713 topsoil samples, developed on the above parent materials, (0–20 cm) were collected from the surface using a regular 1 × 1 km grid (Fig. 1), including 1829 sample for quaternary sediments, 1008 for basalt, 802 for sedimentary rocks, 3966 for granite, 1108 for metamorphic rock. To minimize sampling errors, each sample weighing ca. 1.0 kg was composed of four sub-samples within each 1 × 1 km sampling cell. At the same time, a total of 2197 subsoil samples (150–200 cm) were also gathered based on a 2 × 2 km grid, basically at the center of a group of 4 topsoil samples (Fig. 1), including 484 samples for quaternary sediments, 255 for basalt, 198 for sedimentary rocks, 987 for granite, 273 for metamorphic rock. Either for the topsoil or for the subsoil, samples were collected with 5% field-sampling duplicates.

To avoiding post-contaminants, samples were collected by a stainless drill, and stored in a leaned package. All the soils were air-dried and passed through a 70 mesh sieve. After that, approximately 200 g of each sample was ground in an agate mortar, sieved through a 100 mesh sieve, and then stored at 4 °C for chemical analysis.

2.2. Analytic methods and quality control

Chemical analyses were carried out according to National Standard Soil Environmental Quality Standards in China (GB 15618-2008). The elements of Cd, Co and Cu were analyzed using inductively coupled plasma mass spectrometry (ICP-MS, 6020A), while Cr, Pb and Zn were analyzed using X-ray fluorescence spectrometry (RS-1818, HORNGJAAN). Mercury (Hg) and As were analyzed with anatomic fluorescence spectrophotometer (XGY-1011A). For quality assurance and quality control (QA/QC), standard reference materials GSS-1 and GSS-4 were used as part of the QA/QC procedures, which were obtained from the Center of National Standard Reference Material of China. Satisfied agreement was achieved between the data gained from the present work and the certified values, with recoveries between 92 and 106%. Analysis of the samples, including soil samples and blanks, were performed in triplicate and the standard deviation was within 5%. Also, 7% blind duplicates were analyzed to check the analysis quality. Also, the 2% field-sampling duplicates were checked to be satisfied.

2.3. Statistical analysis and geochemical mapping

Descriptive statistics data are shown in Table S1, including the arithmetic mean, median, maximum, minimum, standard deviation and coefficient of variation (CV), which was respectively calculated for topsoil and subsoil samples from the five related parent material area by means of SPSS 19.0 software. Exploratory data analysis was run to generate histograms and box-plots to support the statistical description of data. The Kolmogorov–Smirnov test, including skewness and kurtosis were applied to assess normality of the distribution of data set.

In correspondence with the location of each subsoil site, the value reported by the interpolated map of topsoils was assumed as concentration for the surface soils. The Pearson's correlation analysis was performed to determine the strength of a linear relationship between PTEs in topsoil and in subsoil. Among numerous kriging techniques, ordinary kriging is one of the most familiar interpolation methods to map the spatial distributions of PTEs (Zhao et al., 2010b; Li et al., 2014). MapGis 6.7 software was used to map the distribution of elements by using ordinary kriging interpolation, and ten intervals were tentatively assigned to divide the concentration in order to show the spatial change of the concentration not only in detail but also concisely.

To discriminate the effect on the loss or enrichment of PTEs in topsoil, the CEF (Ansari et al., 2000; Fergusson, 1990) was applied. Considering the value of its CV and the differences between the topsoil and subsoil, the element scandium (Sc) shows the less variable among the others within the data set and appeared more stable against the weathering loss (Table S1, Fig. S1). In order to reduce the influence of

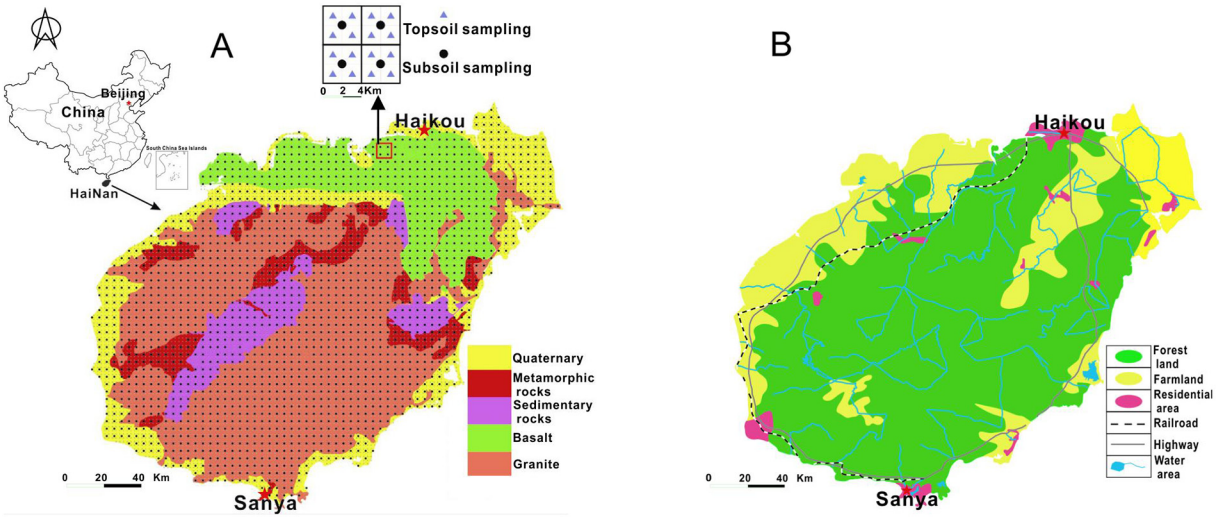

Fig. 1. Lithological distribution and sampling sites in Hainan Island (A), and land use types in Hainan Island (B).

the environmental medium, Sc was used as a normalizing reference element in accordance with the above results on elemental variability. CEF was calculated for each element as following Eq. (1) (Fergusson, 1990):

$$CEF = \frac{(C_i/C_{Sc})_{Topsoil}}{(C_i/C_{Sc})_{Subsoil}} \quad (1)$$

where C_i is the interpolated map of the i-esim PTE in topsoil and in subsoil;

C_{Sc} is the interpolated map of the reference element (Sc) in topsoil and subsoil.

To check out potential pollution or loss of each PTEs in the study area, spatial distribution of CEF for 8 PTEs was estimated by ordinary kriging and mapped with the MapGis 6.7. Based on above calculation, CEF values were divided into five levels as following reported method (Sutherland, 2000): CEF < 2 (No or low pollution); 2 < CEF < 5 (Moderate potential pollution); 5 < CEF < 20 (High potential pollution); 20 < CEF < 40 (Very high potential pollution); 40 < CEF (Extreme potential pollution).

2.4. Geostatistical analysis of variography

Geostatistical methods are based on the theory of regionalized variables (Matheron, 1963), which has been applied to predict the distribution of geochemical variables across unsampled areas assuming that closer samples are more correlated than the farer ones (Chen et al., 2009; Qishlaqi et al., 2009). Kriging has been extensively applied as an important interpolation method at different scales, especially in geochemical studies (Chen et al., 2008; Zhao et al., 2010a). In our case, the concentrations (after logarithmic transformation) of the eight PTEs in the topsoil of Granite area (almost half of the Hainan Island area) were selected to calculate the autocorrelation value to produce a minimum unbiased variance estimate (Qishlaqi et al., 2009). The experimental semivariance was calculated by using the Matheron's classical estimator by the following Eq. (2):

$$\gamma(h) = \frac{1}{2N(h)} \sum_{i=1}^{N(h)} [Z(x_i) - Z(x_i + h)]^2 \quad (2)$$

where $Z(x_i)$ is the value of Z at location x_i, and $Z(x_i + h)$ is the value of Z at a location apart from x_i by distance h, and N(h) is the number of pairs of separated by h. There was no obviously anisotropy in semivariograms of PTEs in different directions. Therefore, isotropic models were tried to fit to the data set of each PTEs, and to auto-fit one of the models (spherical, exponential, Gaussian, linear), and then select the best matching one. Each of the model can be depicted based on three parameters: nugget variance (C_0) for the y-intercept of the model, sill ($C_0 + C$) for the asymptote, and range (A_0) for the obviously distance over spatial dependence (Matheron, 1963; Kashem and Singh, 2001). The model was selected on the basis of the regression coefficient of determination (R^2) and residual sum of squares (RSS) (Li et al., 2014). The best-fitted theoretical model for an experimental semivariogram could be chosen by the highest R^2 value, and the fitted one was used to analyze the spatial structure (Li et al., 2014). In this model, the ratio of nugget to sill ($C_0/(C_0 + C)$) can be considered as standard to define the spatial dependence of soil properties. The ratio higher than 75% suggests the variable with only a weak spatial dependence, between 25% and 75% indicating the variable with moderate spatial dependence, and < 25% manifesting the variable with strong spatial dependence (Liu et al., 2004). In all of this case, exponential model was found to be best-fitted for all 8 PTEs while ordinary kriging was used. All the geostatistical analyses were performed with GS+ (Version 9).

2.5. Compositional and robust biplot analyses

Geochemical data has long been considered as compositional data meaning that the ratio between elements carries more important information than the absolute values (Pawlowsky-Glahn and Bucciani, 2011). Compositional data are vectors of strictly positive real components belonging to the D dimensional simplex space (Aitchison, 1986). Several log-ratio transformations have been elaborated to study the data structure and treat them in the Euclidean space where classical multivariate analysis tools can be applied (Egozcue et al., 2003; Pawlowsky-Glahn and Bucciani, 2011).

One of the most powerful tools to analyze the multivariate compositional data structure is the compositional biplot. This is a two-dimensional graphical display using 2-rank approximation to show both samples (observations) and variables represented by their factor scores and loadings, respectively (Gabriel, 1971). The scores represent the whole covariance structure of the compositional data set in the Euclidian space. The variables are displayed as rays (vectors) from the center of the biplot whose length is proportional to their loadings (the amount of explained variance) in the two-dimensional plane of the first two principal components (Otero et al., 2005; Filzmoser and Hron, 2008; Filzmoser et al., 2009b; Hron et al., 2010). Links between rays refer to the compositional correlation of variables; orthogonal axes indicate uncorrelated variables, rays (vectors) pointing to opposite direction are antithetic elements with respect to each other.

Classical and robust compositional biplot analyses were performed

both on the untransformed and log-transformed (ilr-transformed and clr-backtransformed) topsoil and subsoil data sets to reveal the compositional structure of the investigated variables (natural groupings, correlation) and to better understand the underlying governing factors which explain the compositional variability as much as possible by using principal components. However, the classical biplot based on the covariance matrix of raw-data is substantially influenced by outliers distorting the compositional data matrix and hindering to see the real relationship between parts (variables) and affect the calculation of principal components (Aitchison, 1986; Filzmoser et al., 2009a, 2009b).

In multivariate compositional analysis, the robust version of PCA biplot should be used on log-transformed data with respect to orthonormal basis such as ilr transformed data (Egozcue et al., 2003) and back-transformed to the clr space for the ease of their interpretation. This back transformation preserves the linear relationship between clr and ilr coordinates (Egozcue et al., 2003), using the minimum covariance determinant (MCD) estimator (Rousseeuw and Driessen, 1998). The MCD looks for a subset h out of n observations of the initial data with the lowest determinant of sample covariance matrix (Filzmoser and Hron, 2008) and allow obtaining variables into normal distribution which describe better the correlation or covariance of the data avoiding the outlier artefacts. Classical and robust biplots were made using R statistical open source software.

3. Results and discussion

3.1. PTEs concentration in the topsoil

The histogram plots (Fig. S2) and box-plots (Fig. 2) were plotted for eight PTEs, which can provide a valuable tool for describing various elements distribution (Lu et al., 2012; Mrvić et al., 2011). The mean concentrations of As, Co, Cr, Cu, Pb, Zn, Cd and Hg in topsoils were 5.29, 11.95, 60.79, 17.24, 26.18, 51.22, 0.081 and 0.043 mg/kg (Fig. 2), respectively. It could be observed that, after a log-transformation, As, Pb, Cd and Hg and show a general symmetrical distribution (almost normal, in some cases) while Co, Cr, Cu and Zn are featured by a bimodal trend (Fig. S2) suggesting the presence of two sub-populations. Among the PTEs, Co, Cr, Cu, Pb and Zn have a smaller number of extreme outlier values compared to As, Cd and Hg exhibiting an upward bias distribution with much high and extreme outliers (Fig. 2).

The descriptive statistics were performed for the eight PTEs in topsoil sorted by parent materials. (Table S1). The concentration of Co, Cr and Zn in basaltic soils were 6.20–12.89, 5.51–10.79 and 2.15–4.55 times greater, respectively than those in other 4 soil parent materials, which suggests that lithological geochemistry greatly affected the concentration of PTEs in the soils. Furthermore, concentration of Pb in granitic soils was 36.76 mg/kg, which was much higher than that in other soil parent materials. The concentrations of As and Cd in soils of metamorphic area were 19.76 mg/kg and 0.10 mg/kg, which were 5–8 and 1.5–2.4 times higher than those in other parent material soils, respectively. Although CV values (< 100%) for Co, Cr, Cu, Pb and Zn concentrations were relatively low, those for As, Cd and Hg in 4 parent materials were higher than 100% except in the basaltic soil, which suggests that there exited other impact facts besides of soil parent materials in some areas.

The classic empirical methods eliminating outliers were used to respectively calculate the baseline concentrations of PTEs for the 5 individual parent materials. As shown in Table S1, baseline values for different soil parent materials were significantly different. Generally, values of PTEs in basaltic area are high but low in Quaternary area. The values for Co,Cr,Cu, Zn, Cd and Hg in basaltic area were higher than those in other lithological areas, and times respectively were of 7.30–28.64, 6.70–17.19, 4.22–14.69, 2.30–5.62, 1.27–2.03 and 1.55–1.89. The value of As in the metamorphic soil was of 4.84–7.03 times higher than those in other lithological areas. Pb background value in the granite topsoil was 1.22–2.32 times larger than those in other lithological areas. So, it can be concluded that the type of soil parent material has a great impact on the baseline values of PTEs.

3.2. PTEs concentration in the subsoil

PTEs concentration in the subsoil could be referred to the nature of the original parent materials, and they are seldom influenced by human activities (Reimann et al., 2001). Commonly, PTEs concentrations and distribution in the subsoil represent the lithogenic background.

The box-plots and histograms of PTEs in subsoils are respectively exhibited in Fig. 3 and Fig. S3. In the study area, Cr (65.24 mg/kg) is characterized by the highest mean values (Fig. 3), followed by Zn (58.87 mg/kg), Pb (29.15 mg/kg), Cu (19.97 mg/kg), Co (12.89 mg/kg), As (5.53 mg/kg), Cd (0.065 mg/kg) and Hg (0.029 mg/kg). Except for Cd and Hg, the concentrations of other PTEs in the subsoil are lower than those in the topsoil. Similar to that in the topsoil, most of the PTEs (As, Pb, Zn, Cd, Hg) exhibited a log-normal distribution while Co, Cr and Cu show a bimodal trend (Fig. S3). As summarized in Table S1, the mean concentration of Co (52.46 mg/kg), Cr (234.41 mg/kg), Cu (74.49 mg/kg), Zn (111.25 mg/kg) and Hg (0.047 mg/kg) in basaltic soils were 5.55–7.94, 4.23–6.13, 3.47–6.97 1.72–3.47 and 1.68–1.96 times higher respectively than those in other lithological areas. Concentration of Pb (36.76 mg/kg) in granitic soils was of 1.20–2.32 times larger than those in other lithological soils. Furthermore, the content of As (15.7 mg/kg) and Cd (0.107 mg/kg) in the metamorphic soils were of 3.4–6.1 and 1.6–2.7 times respectively higher than those in other lithological soils.

Usually, the values in the topsoils are higher than those in subsoils due to the superimposed influence of rock-weathering and human activities input on surficial media (Reimann et al., 2001). In this case, as presented in the Table S1, background values of the selected elements (except for Cd and Hg) in the subsoil were generally higher than the

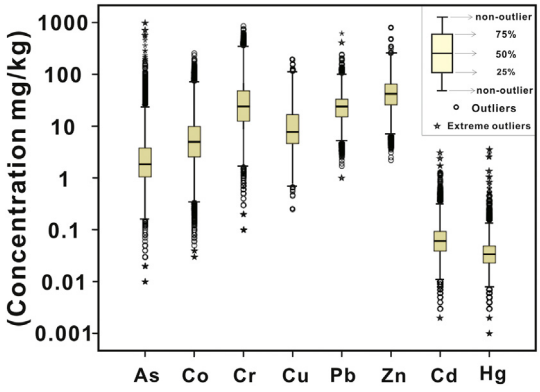

Fig. 2. Box-plot of PTEs concentrations in the topsoil (n, 8713).

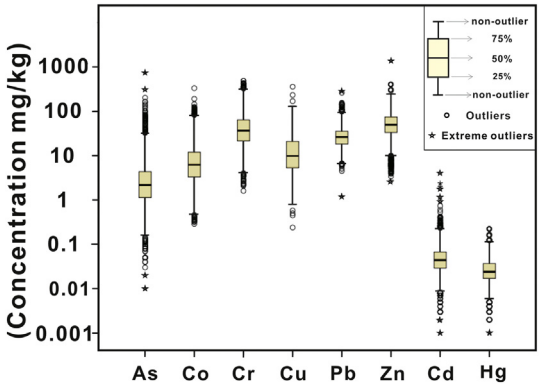

Fig. 3. Box-plot of PTEs concentrations in the subsoil (n, 2197).

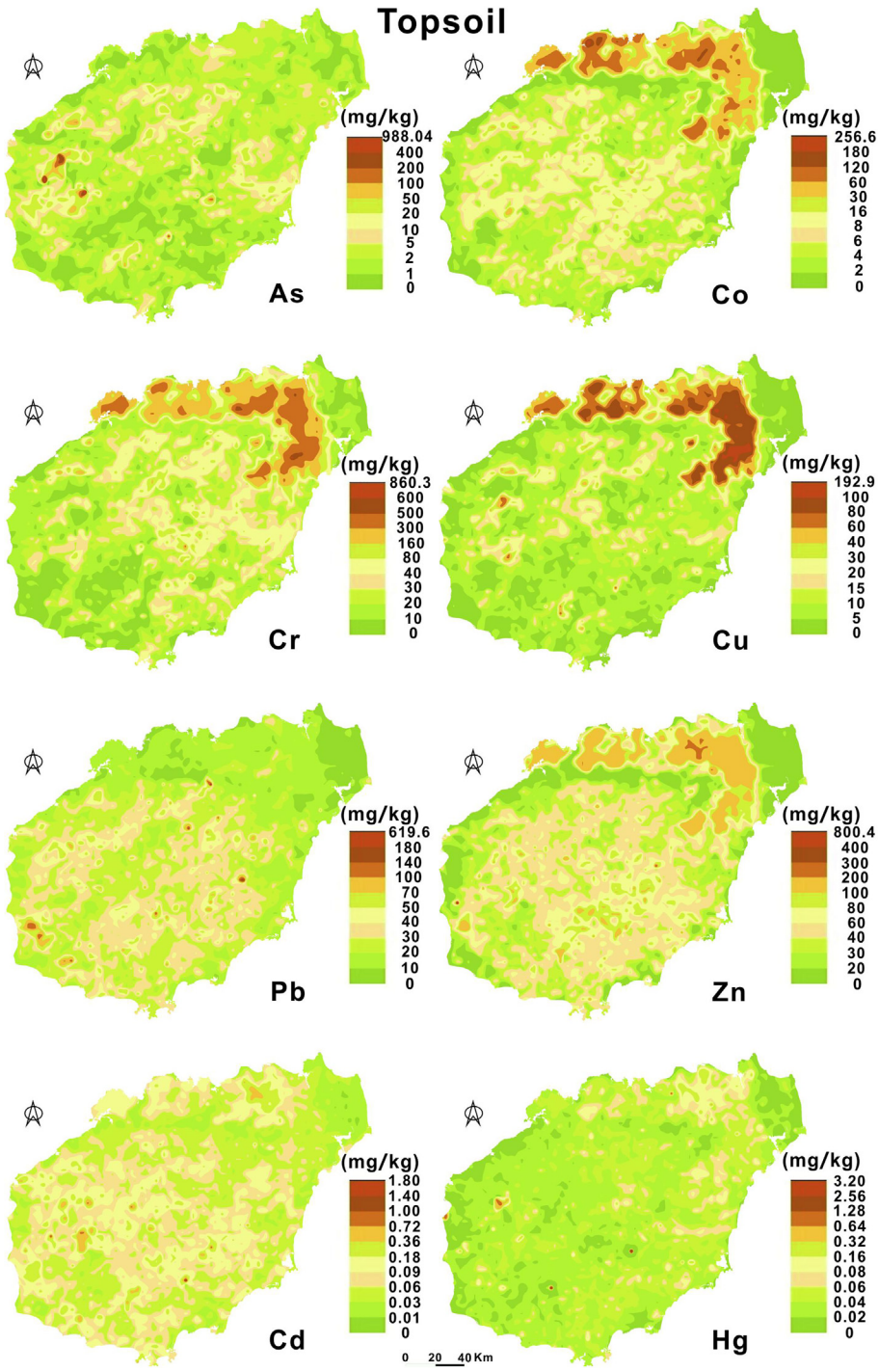

Fig. 4. Spatial distribution of As, Co, Cr, Cu, Pb, Zn, Cd and Hg in the topsoil.

baseline values established from the topsoil. This peculiarity is probably explained by the fact of the location and climate in Hainan Island characterized by a typical tropical marine monsoon with rainy climate, and the weathering in surface is strong enough to leach the topsoil metals as described in Section 2.1.

3.3. Spatial distribution and CEF of PTEs

Topsoil reflects the complex interactions between atmosphere, biosphere and lithosphere, while subsoil generally records the sole contribution of the lithosphere to the surface geochemistry and can be used to state the geogenic background level for elements (Reimann et al., 2001). Distribution patterns of PTEs concentrations in topsoils and subsoils (Fig. 4 & Fig. 5) were mapped. Particularly for Cd and Hg, the sites of high values in the topsoil were distinctly different from that in the subsoil. Presumably, some anthropogenic activities may affect the spatial distribution of Cd and Hg in topsoil, which were obviously different from others (Fig. S2). Many previous studies reported that Cd and Hg in the soil of China were significantly related with the rapid urbanization for decades (Sun et al., 2010). Furthermore, Hg pollution in urban soil was very universal in China, which usually originated from the fossil fuel combustion and atmospheric deposition (Wang et al., 2003; Kuo et al., 2006).

Either in the topsoil or in the subsoil, spatial distribution of As, Co,

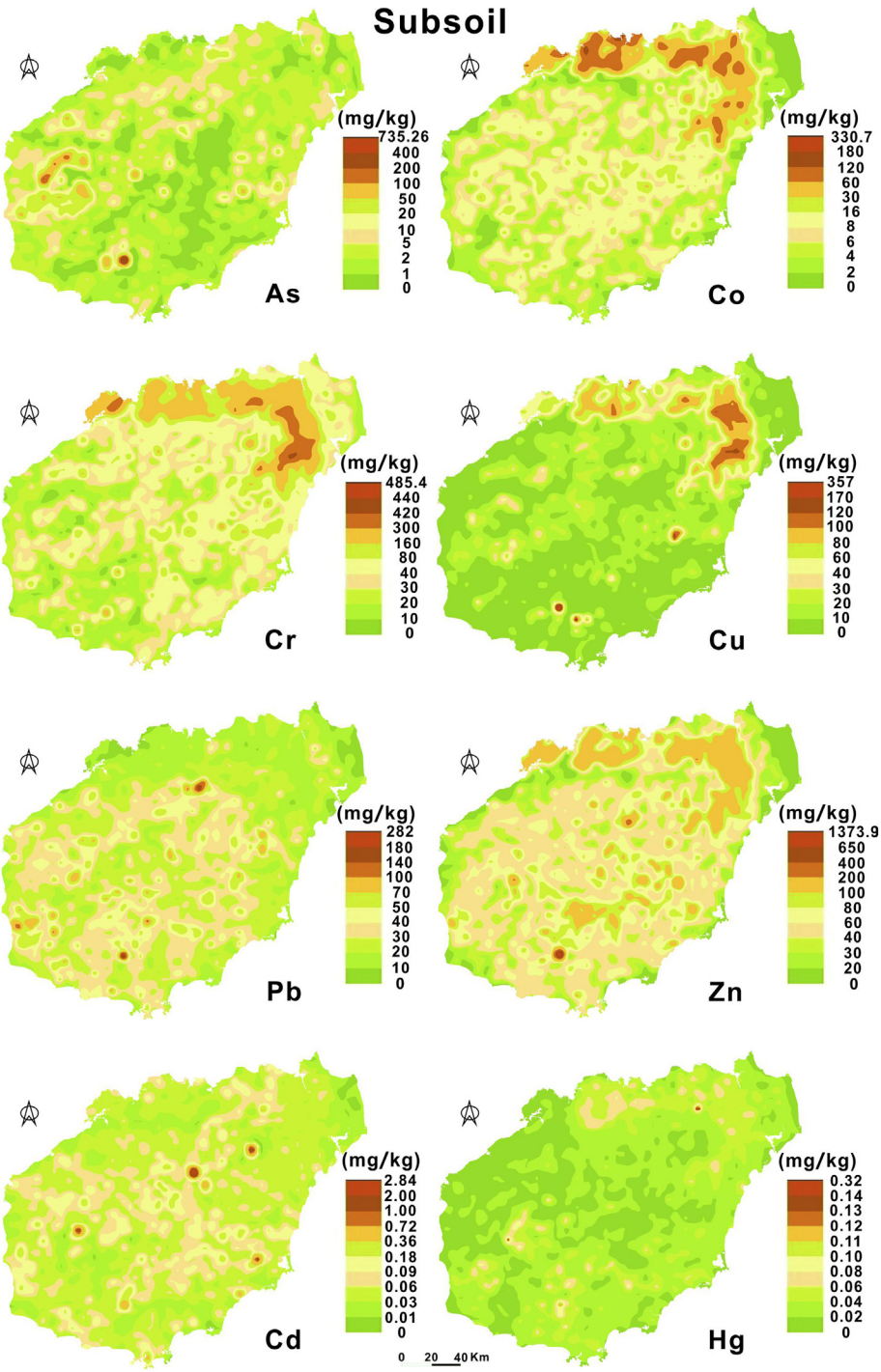

Fig. 5. Spatial distribution of As, Co, Cr, Cu, Pb, Zn, Cd and Hg in the subsoil.

Cr, Cu, Pb and Zn was remarkably similar. Possibly, the spatial variation of their contents was primarily influenced by the distribution of soil parent materials in the regional scale (Zhang et al., 2008). In most of the areas, the mean concentration of As was lower than 50 mg/kg either in the topsoil or in the subsoil, while some higher values was observed in the area of Mesozoic sedimentary rock. The concentrations of Co, Cr, Cu and Zn in area of the basalt were distinctly higher than those in other lithological areas. So, the accumulation of elements in the soil mainly resulted from the pedogenesis from rocks, while the later anthropogenic activities may influence the spatial variability of Cd and Hg in the topsoil.

At the regional scale, the major influence factors on PTEs distribution in the topsoil were variations in parent material of geology, weathering and various anthropogenic sources (Reimann et al., 2001). The majority of CEF values for most of PTEs, such as As, Co, Cr, Cu, Pb and Zn, are mainly < 2 (Fig. 6). This result indicates that the main source of them in the topsoil was mainly originated from soil parent materials without potential pollution in the study area, expecting a few sites for As. For Cd and Hg, CEF values in some sites is higher than 2 but < 5, suggesting that Cd and Hg posed a moderate potential contaminate at some areas. The relative low CEF values for As, Co, Cr, Cu, Pb and Zn may be due to strongly weathering resulted in leaching a large number of elements in the topsoil without anthropogenic input pollution. In contrast, the relatively high CEF values for Cd and Hg

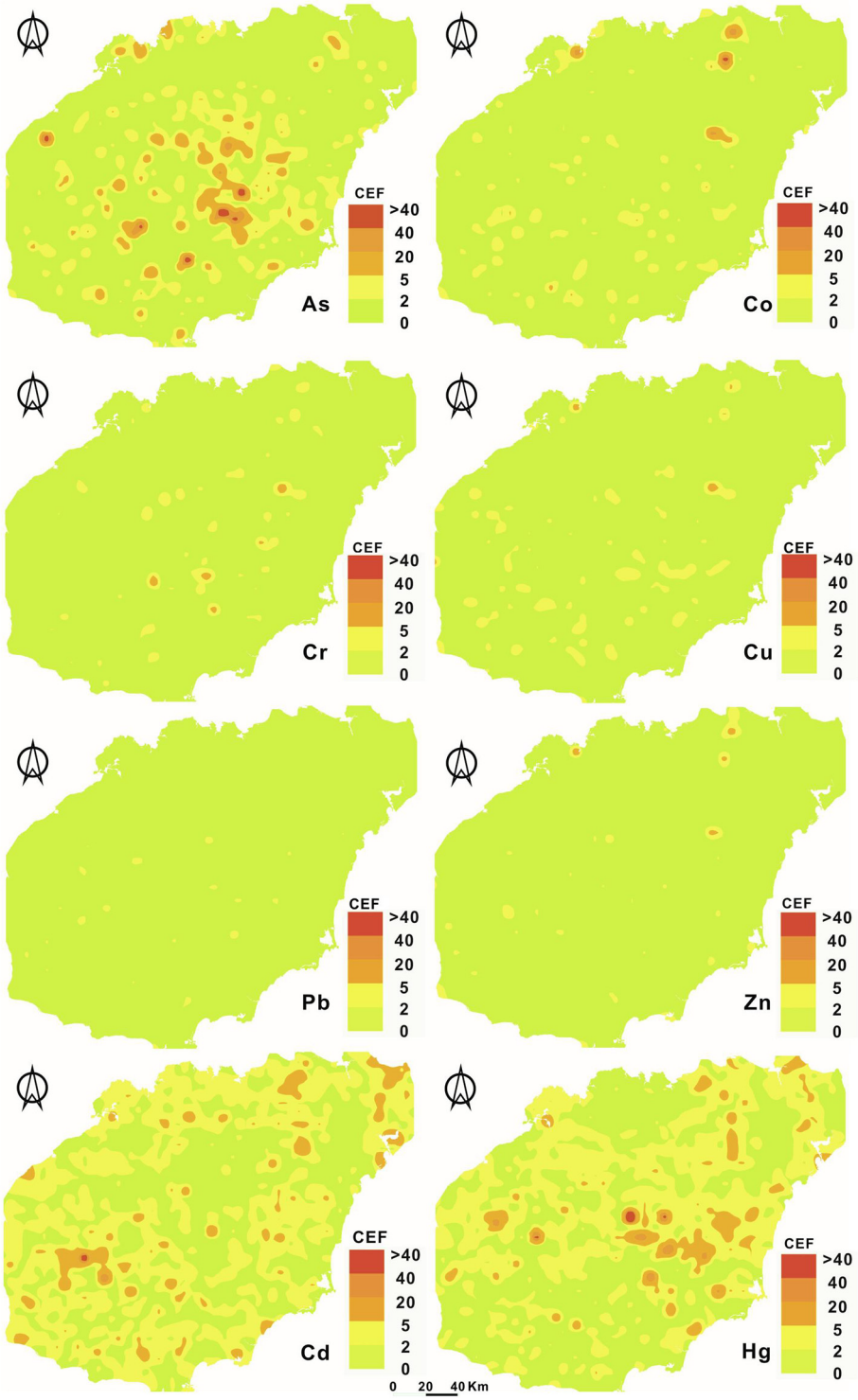

Fig. 6. Spatial distribution of CEF values for PTEs in the soil.

manifest that topsoils may be contaminated by human activities from sites to sites (Fig. 1B).

3.4. Pearson correlation analysis

PTEs in the topsoil show a certain inheritance from the subsoil. To investigate their relationship, Pearson's correlation analysis was conducted and the results of correlation coefficients were listed in Table 1. A significantly positive correlation was respectively found for As, Co, Cr, Cu, Pb and Zn at significance level (correlation coefficient between 0.51 and 0.79, $P < 0.01$), which suggests that these metals in topsoil mainly inherited from the subsoil (geological background) and were seldom disturbed by human activities or other input sources. However, in all kinds of rocks area, either Cd or Hg in the topsoil does not significant correlate with that in the subsoil (Table 1), which indicate Cd and Hg in the topsoil were possibly affected by human activities, such as vehicle emissions, industrial and agricultural activities at some areas (Fig. 1B).

Table 1
Pearson correlation coefficients for PTEs between in the topsoil and in the subsoil of 5 lithological areas.

Elements	Pearson correlation coefficients				
	Quaternary soils	Basalt soils	Sedimentary rocks soils	Granite soils	Metamorphic rocks soils
As	0.68**	0.77**	0.58**	0.63**	0.64**
Co	0.79**	0.58**	0.57**	0.56**	0.55**
Cr	0.73**	0.72**	0.70**	0.51**	0.53**
Cu	0.75**	0.77**	0.61**	0.58**	0.62**
Pb	0.63**	0.55**	0.54**	0.66**	0.52**
Zn	0.65**	0.62**	0.53**	0.53**	0.53**
Cd	0.38**	0.39**	0.16*	0.34**	0.10*
Hg	0.25*	0.17*	0.12*	0.12*	0.05

** Correlation is significant at the 0.01 level.
* Correlation is significant at the 0.05 level.

3.5. Multivariate analysis of variography for PTEs in topsoils of granitic area

In this case, variogram analysis was carried out to further confirm above discussion. Since granite is the most widely distributed lithology in Hainan Island (Fig. 1), the features of the semivariograms for As, Co, Cr, Cu, Pb, Zn, Cd and Hg in topsoils of granitic area were selected representatively and summarized in Table 2. It appears that the semivariograms parameters (the best fit model types, nugget, sill, effective range and nugget to sill ratio) are different for the 8 PTEs.

Of which, As, Co, Cr, Cu, Pb and Zn were characterized by relatively low nugget to sill ratio (5.8–24.5%) and long effective range (75,200 m–132,247 m). These metals were all best-fitted to the exponential model (Fig. 7) with relatively high coefficient of determination (0.752–0.972). As shown in Table 2, the strong spatial dependence is found for As, Co, Cr, Cu, Pb and Zn in the topsoil. The continuous variation with a large effective range indicates the continuity of the spatial distribution of PTEs. It is well known that Cr and Co are typical lithogenic elements. The mean concentrations of Pb and Zn in the topsoil was almost completely closed to their corresponding background value (Table S1), which suggest elements in the topsoil mainly originated from the lithogenic source without obvious human activities input (Gilg et al., 2006). Evidently, the spatial variability of As, Co, Cr, Cu, Pb and Zn were mainly affected by intrinsic factors, in which the parent material and subsequent pedogenic process were dominant influence factors on elements (Micó et al., 2006; Rodríguez et al., 2008).

As shown in Fig. 7 and Table 2, Cd and Hg show relatively high ratio of nugget to sill (75.6%–77.2%) and small effective range (9100 m~14,174 m) while fitted to the exponential model. The weak spatial dependence for the Cd and Hg suggests that the spatial distribution of the two elements was affected by extrinsic factors, such as traffic or other human activities. Declaring briefly, there might exit small scale correlation appeared at intervals less than the distance between sampling sites, which cannot be detected with the dataset in this case. Through semivariogram analysis, the spatial variations of PTEs in the topsoil show two distribution patterns at the regional scale, intrinsic (As, Co, Cr, Cu, Pb and Zn) and exogenous (Cd and Hg) variability. These results agree with the distribution patterns and CEF values as discussed above.

3.6. Multivariate compositional data analysis for the topsoil

Classical compositional and robust compositional biplot analyses were performed on untransformed and log-transformed (ilr-transformed and clr-backtransformed) subsoil and topsoil data sets to reveal the compositional structure of the investigated variables (natural groupings, correlation) and explain the compositional variability as much as possible by using principal components.

The first two principal axes of the classical biplot based on topsoil raw-data explain 64.42% cumulative total variability (PC1: 42.28%, PC2: 22.14%) (Fig. 8A). The direction of parts (variables) and their coefficients (loadings) are strongly biased toward two distinct associations of elements which are totally uncorrelated proven by the almost right angle between the variable axes (Fig. 8A). One group includes Co, Cr, Cu and Sc and all of them have similar positive loadings (0.44–0.46). They may be related to the presence of mafic rocks (basalt) because the scores of samples from soils over basalt parent material are all distributed around this group. The other association is composed of As, Pb, Cd and Hg and they all have negative loadings in the PC2 axis. The highest negative loadings are related to Pb and Cd (-0.54, -0.55), the smallest one (-0.33) belongs to Hg (Fig. 8A). This group is not unambiguously associated with one typical lithology but granite and metamorphic samples with high dispersion are mainly concentrated around these elemental axes. In general, these elements are more enriched in granites and felsic rocks compared to mafic and ultramafic rocks (Wedepohl, 1978; Fergusson, 1990; Ottensen et al., 2013). Hg and Cd are deemed to be influenced by anthropogenic contamination in the study area, but the classical biplot based on the raw-data is unable to capture it. Zn is located separately and might indicate a transition character between the two large groups of elements (Fig. 8A). The classical PCA biplot does not capture the real compositional structure and relations between the variables due to the presence of outliers and the strong bias toward the large parent material groups (e.g. granite). In addition, the data structure is distorted which is indicated by the curve-

Table 2
The parameters and the best fitted variogram models for PTEs in granite soils.

Elements	Best fit model	Nugget (C_0)	Sill (C_0 + C)	Range (m)	$C_0/(C_0 + C)$	R^2	RSS
As	Exponential	0.251	1.033	75,200	0.243	0.937	9.303E−03
Co	Exponential	0.035	0.553	123,112	0.058	0.752	0.0232
Cr	Exponential	0.34	1.39	132,247	0.245	0.972	0.0107
Cu	Exponential	0.105	0.436	114,074	0.241	0.884	4.556E−03
Pb	Exponential	0.048	0.201	132,172	0.239	0.873	1.805E−03
Zn	Exponential	0.055	0.252	124,024	0.202	0.964	2.433E−04
Cd	Exponential	0.0037	0.0048	9100	0.772	0.886	4.046E−07
Hg	Exponential	0.21	0.278	14,174	0.756	0.838	4.532E−03

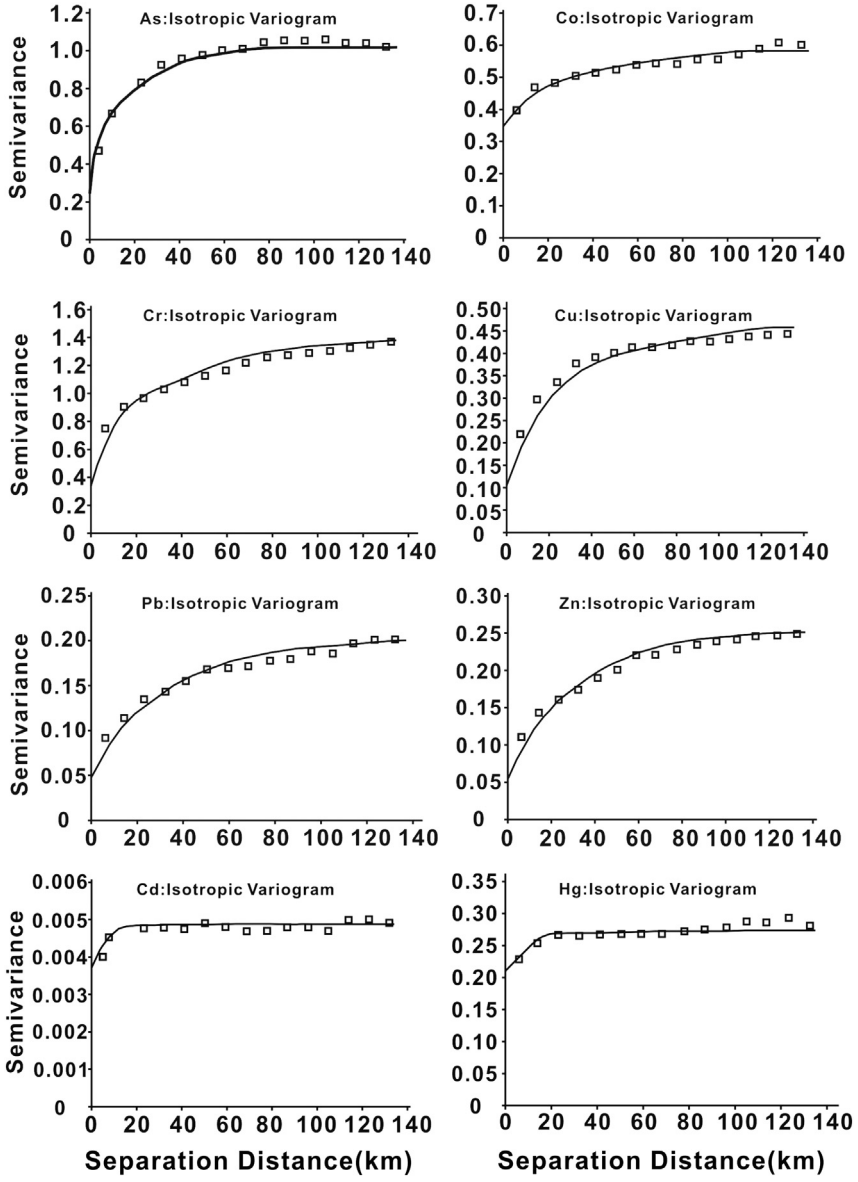

Fig. 7. Experimental variogram and the best fitted variogram models for PTEs in topsoils of granitic area.

shaped configuration of factor scores which hinder to reveal their compositional behavior.

In contrast, the first two principal axes of the robust PCA biplot based on the log-transformed (ilr-transformed and clr-backtransformed) topsoil data set captures 72.38% total cumulative variability (PC1: 44.13%, PC2: 28.25%) which almost 10% higher than the classical one's (Fig. 8B). The robust biplot is less contaminated by outliers; hence the real relations between compositional parts can be clearly studied. The biplot enhances and separates much better the different soil parent materials and their related elemental associations. The Mesozoic sediments are the most representative samples and they show the least element variability because their scores are all located at the intersection of the two principal axes (Fig. 8B). The highest factor scores (outliers) belong to samples over granite and basalt parent materials showing their high compositional variance in terms of the 9 investigated elements.

The highest compositional variability is related to As element based on its highest negative loading (−0.75) on the PC1 axis (Fig. 8B). The CV (Coefficient of Variation) of As exceeded 100% both in case of subsoil and topsoil samples. Arsenic belonged to the element association of Cd, Hg and Pb in the classical biplot, but the robust method clearly separates it. The highest As concentration was measured in soils over metamorphic parent material. The factor scores of samples from soils over metamorphic rocks are concentrated all around the axes of As which confirms the strong lithological control on As distribution (Fig. 8B). However, the highest loading of As might be also related to its changeable mobility in surface environment influenced by pH, Eh, the presence of organic matter, clay minerals and secondary iron-oxy-hydroxides (Kabatapendias, 2010; Reimann and Garrett, 2005; Tarvainen et al., 2013). It can accumulate under alkaline environment (pH: 7–9) in strongly weathered 'terra rossa' soils but low pH and Eh conditions favors its mobility (Kabatapendias, 2010). However, we cannot exclude the anthropogenic contamination as a contributor to its variability especially in the central urbanized area of Hainan Island (CEF, 2–5).

Cd, Hg and Pb indicate a second group with high positive loadings on the PC1 and PC2 axes (Fig. 8B). The highest and lowest loadings are related to Pb (PC1: 0.38, PC2: 0.36) and Hg (PC1: 0.12, PC2: 0.22), respectively. The variation of these elements is also influenced by lithological control, especially in case of Pb whose concentration was the highest over granite parent material. In case of Cd and Hg distribution, we demonstrated a superposition of anthropogenic contamination on

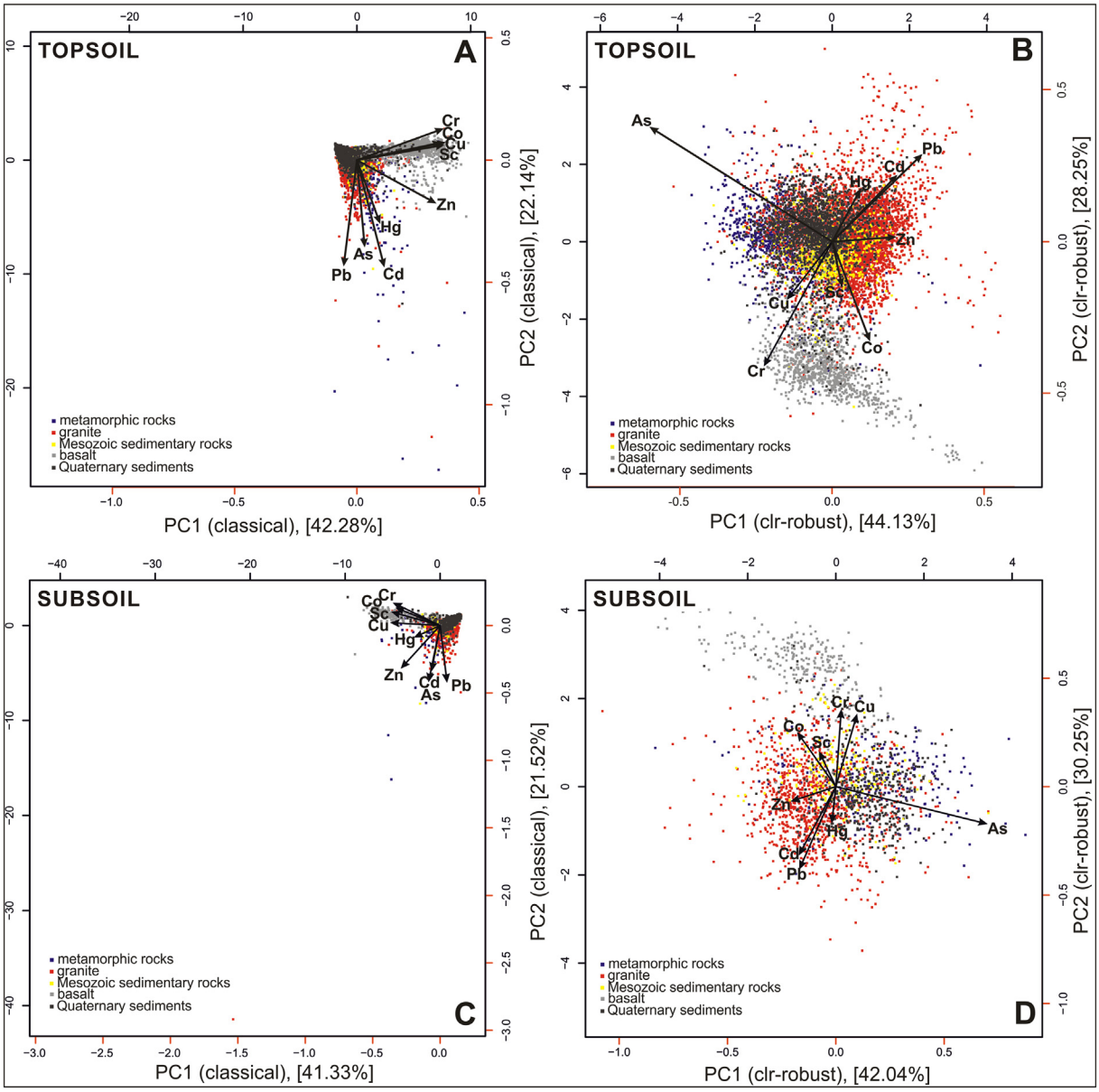

Fig. 8. The compositional classical biplots of raw topsoil and subsoil data (A, C) and the robust biplots of log-transformed topsoil and subsoil data (B, D).

lithological control proven by their higher topsoil concentration with respect to subsoil, different spatial pattern for subsoil and topsoil, large nugget to sill ratio (> 75%) and their low Pearson correlations (R < 0.4) between subsoil and topsoil data. The highest topsoil/subsoil concentration ratios were reported for Cd, Pb and Hg in the Europen FOREGS (Forum of European Geological Survey) data set (Salminen et al., 2005). It was explained by the combination of anthropogenic contamination (e.g. smelting industry, traffic), the higher organic matter contents (e.g. organic compounds: Cd, Hg) in surface topsoil, repeated reprecipitation (e.g. Cd) and rainfall control (e.g. Hg). This group of elements may indicate the anthropogenic contamination factor (e.g. heavy traffic) which was superimposed on lithological control of granite and metamorphic parent materials. This might be confirmed by their similar positive loadings both on the PC1 and PC2 axes (Fig. 8B). In case of Pb, the lithological control (granite parent material) was much more enhanced proven by its higher subsoil concentration.

The third group is composed of Co, Cr, Cu and Sc and represented by strong negative loadings along the PC2 axis (Fig. 8B). They are the antithetic elements of Cd, Pb and Hg. The highest and smallest loadings are related to Cr (−0.52) and Sc (−0.2), respectively. The biplot clearly distinguishes the important lithological control on this group, because factor scores of samples deriving from basalt parent material are located all around these elements (Fig. 8B). All of them indicate the presence of mafic parent materials which are generally enriched in these elements during early magmatic fractionation due to their high compatibility (Reimann et al., 2014). This group reflects geogenic control on spatial distribution of this element association. Zn is a transitory element between the two main large elemental associations (Group 2 and 3) (Fig. 8B). They have higher concentration in subsoil than in topsoil and its CEF values were below 2; hence its spatial variability is mainly governed by geogenic factors. Zn is not related to a specific soil parent material and its transition character might be explained by its less affinity to a particular lithology and its different mobility with respect to other elemental associations.

3.7. Multivariate compositional data analysis for the subsoil

The classical and robust PCA biplot analyses performed on subsoil data enhance much better the geogenic factors (e.g. soil parent material) governing the spatial variability of the compositional data set.

Subsoil data are less affected by anthropogenic contamination and weathering; hence they reflect the geology underneath (Reimann et al., 2001). The classical PCA biplot for subsoil raw data reveals similar features to those depicted by topsoil data set. The first two axes explain 62.85% cumulative total variability (PC1: 41.33%, PC2: 21.52%). However, the classical biplot is strongly biased toward the same two groups of elements (Group1: Co, Cr, Cu, Sc; Group2: As, Cd, Pb) as was in the case of topsoil data and the factor scores are heavily distorted and have curve-shaped configuration preventing us from seeing the real compositional structure (Fig. 8C). The magnitude of loadings is similar, the only difference is that Hg has been removed from the Group2 and placed closer to the Group1 elements (Fig. 8C).

In contrast, the robust PCA biplot based on log-transformed subsoil data "opened" the real data structure and its two principal axes explain higher (72.29%) cumulative total variability (PC1: 42.04%, PC2: 30.25%) (Fig. 8D). The same groups of elements with similar magnitude of loadings can be observed on the robust PCA biplot as we could see in case of topsoil data (Fig. 8D). This means that the main governing factor for compositional elemental associations is the soil parent material in the Hainan Island. Factor scores are also similar to those of topsoil; the most representative samples with smallest variability derive from soils over Mesozoic sedimentary rocks. The highest factor scores are related to samples from basaltic soil because they are the farthest from the intersection of two main principal axes (Fig. 8D). The highest variability represented by As with the highest positive loading (0.85) on the PC1 axis. They are mainly surrounded by samples from soils over metamorphic parent material. The second group contains Cd, Hg and Pb and they were related to the superposition of lithological and anthropogenic effect (Fig. 8D). However, the similar loadings and natural grouping on the robust topsoil and subsoil biplots suggest a stronger lithological impact on their spatial distribution. The third group is represented by the indicator elements of mafic rocks (Co, Cr, Cu and Sc) which are antithetic with Cd, Hg and Pb. They have positive loadings on the second principal axes and related to basalt parent material (Fig. 8D). Zn is displayed as a transitory element, antithetic with As which has negative loading on the PC1 axes. Its transition character cannot be explained by its less affinity to a particular lithology and its different mobility with respect to other elemental associations (Fig. 8D).

4. Conclusions

In Hainan Island, the element concentrations of As, Co, Cr, Cu, Pb and Zn in the topsoil were slightly lower than those in the subsoil, while Cd and Hg were different. Spatial distribution patterns of As, Co, Cr, Cu, Pb and Zn concentration in the topsoil are remarkably similar to those in subsoil. The values of CEF for Cd and Hg are between 2 and 5 in soil profiles, suggesting that superposition of anthropogenic inputs on soil parent materials. The positive relationship (coefficients, 0.51–0.79) was found for PTEs between the topsoil and the subsoil in all kinds of lithology, indicating the dominant impact of soil parent materials. The strong spatial dependence for As, Co, Cr, Cu, Pb and Zn by semivariograms analysis suggests that their variables were mainly resulted from intrinsic variability, which refers to soil parent materials associated with geological rocks. On the other hand, exogenous variability may be superposed on Cd and Hg which refers to anthropogenic inputs. Multivariate compositional data analysis was performed for PTEs both in the topsoil and in the subsoil, which were divided into four groups in the topsoil: the first of Cd, Hg and Pb, the second of Co, Cr, Cu and Sc, the third of As and the forth of Zn. All of them were superposed by lithological or anthropogenic effect.

Acknowledgements

National Nautural Science Foundation (41372249, 41872100) and the Fundamental Research Funds for the Central Universities (2652017240) in China financially supported this research. We are grateful to Hainan Geological Survey Institute for kind support of data collection.

Appendix A. Supplementary data

Fig. S1, The spatial distribution of Sc in the topsoil and subsoil; Table S1, summary statistics of PTEs in the topsoil and in subsoil based on 5 soil parent materials; Fig. S2, histograms for PTEs in the topsoil; Fig. S3, histograms for PTEs in the subsoil. Supplementary data to this article can be found online at https://doi.org/10.1016/j.gexplo.2018.11.008.

References

Acosta, J.A., 2011. Accumulations of major and trace elements in particle size fractions of soils on eight different parent materials. Geoderma 161, 30–42.
Adot, E.L., Sánchez-Carpintero, P., Reixach, J.G., Valencia, D.E., 2006. Geochemical inheritance of soils that develop from volcanic rocks (Navarra, Western Pyrenees). Geoderma 135, 38–48.
Aitchison, J., 1986. The Statistical Analysis of Compositional Data. Chapman and Hall, London-New York, pp. 416.
Alary, C., Demougeot-Renard, H., 2010. Factorial kriging analysis as a tool for explaining the complex spatial distribution of metals in sediments. Environ. Sci. Technol. 44, 593–599.
Albanese, S., De Vivo, B., Lima, A., Cicchella, D., 2007. Geochemical background and baseline values of toxic elements in stream sediments of Campania region (Italy). J. Geochem. Explor. 93, 21–34.
Ansari, A.A., Singh, I.B., Tobschal, H.J., 2000. Importance of geomorphology and sedimentation processes for metal dispersion in sediments and soils of the Ganga Plain: identification of geochemical domains. Chem. Geol. 162 (3), 245–266.
Bini, C., Sartori, G., Wahsha, M., Fontana, S., 2011. Background levels of trace elements and soil geochemistry at regional level in NE Italy. J. Geochem. Explor. 109, 125–133.
Chen, T., Liu, X., Zhu, M., Zhao, K., Wu, J., Xu, J., Huang, P., 2008. Identification of trace element sources and associated risk assessment in vegetable soils of the urban–rural transitional area of Hangzhou, China. Environ. Pollut. 151 (1), 67–78.
Chen, T., Liu, X., Li, X., Zhao, K., Zhang, J., Xu, J., Dahlgren, R.A., 2009. Heavy metal sources identification and sampling uncertainty analysis in a field-scale vegetable soil of Hangzhou, China. Environ. Pollut. 157 (3), 1003–1010.
Egozcue, J.J., Pawlowsky-Glahn, V., Mateu-Figueraz, G., Barceló-Vidal, C., 2003. Isometric logratio transformations for compositional data analysis. Math. Geol. 35 (3), 279–300.
Environmental Quality Standards for Soils of China. GB 15618-2008.
Facchinelli, A., Sacchi, E., Mallen, L., 2001. Multivariate statistical and GIS-based approach to identify heavy metal sources in soils. Environ. Pollut. 114 (3), 313–324.
Fergusson, J.E., 1990. The Heavy Elements: Chemistry, Environmental Impact and Health Effects. Pergamon Press, New York, pp. 412.
Filzmoser, P., Hron, K., 2008. Outlier detection for compositional data using robust methods. Math. Geosci. 40 (3), 233–248.
Filzmoser, P., Hron, K., Reimann, C., 2009a. Principal component analysis for compositional data with outliers. Environmetrics 20 (6), 621–632.
Filzmoser, P., Hron, K., Reimann, C., 2009b. Univariate statistical analysis of environmental (compositional) data: problems and possibilities. Sci. Total Environ. 407 (23), 6100–6108.
Frattini, P., De Vivo, B., Lima, A., Cicchella, D., 2006. Elemental and gamma-ray surveys in the volcanic soils of Ischia island, Italy. Geochem. Explor. Environ. Anal. 6 (4), 325–339.
Fu, Y.R., Chen, M.L., Bi, X.Y., He, Y.H., Ren, L.M., Wu, X., Qiao, S.Y., Yan, S., Li, Z.G., Ma, Z.D., 2011. Occurrence of arsenic in brown rice and its relationship to soil properties from Hainan Island, China. Environ. Pollut. 159 (7), 1757–1762.
Gabriel, K.R., 1971. The biplot graphic display of matrices with application to principal component analysis. Biometrika 58 (3), 453–467.
Gilg, H.A., Boni, M., Balassone, G., Allen, C.R., Banks, D., Moore, F., 2006. Marble-hosted sulfide ores in the Angouran Zn–(Pb–Ag) deposit, NW Iran: interaction of sedimentary brines with a metamorphic core complex. Mineral. Deposita 41 (1), 1–16.
Gong, C., Ma, L., Cheng, H., Liu, Y., Xu, D., Li, B., Liu, F., Ren, Y., Liu, Z., Zhao, C., Yang, K., Nie, H., Lang, C., 2014. Characterization of the particle size fraction associated heavy metals in tropical arable soils from Hainan Island, China. J. Geochem. Explor. 139, 109–114.
Hanesch, M., Scholger, R., Dekkers, M.J., 2001. The application of fuzzy C-means cluster analysis and non-linear mapping to a soil data set for detection of polluted sites. Phys. Chem. Earth 26 (11), 885–891.
Hao, L.H., Zhang, D.M., Wu, P.F., Dai, Y., Qi, Z.P., 2009. Spatial distribution of PTEs content in the farmlands of Hainan Island. China J. Eco-Agr. 17 (2), 230–234 (With abstract in English).
Hron, K., Templ, M., Filzmoser, P., 2010. Imputation of missing values for compositional data using classical and robust methods. Comput. Stat. Data Anal. 54 (12), 3095–3107.
Kabatapendias, A., 2010. Trace Elements in Soils and Plants, Fourth edition. Crc Press.
Kashem, M.A., Singh, B.R., 2001. Metal availability in contaminated soils: I. Effects of

flooding and organic matter on changes in Eh, pH and solubility of Cd, Ni and Zn. Nutr. Cycl. Agroecosyst. 61 (3), 247–255.
Kuo, T.H., Chang, C.F., Urba, A., Kvietkus, K., 2006. Atmospheric gaseous mercury in Northern Taiwan. Sci. Total Environ. 368 (1), 10–18.
Li, F.Y., Li, X.M., Wu, P.F., Chen, L.Y., Guo, B., Qi, Z.P., 2009. Correlation between heavy metal pollution and basic properties of agricultural soils in Hainan Province. Soil 41 (1), 49–53 (in Chinese).
Li, W.L., Xu, B.B., Song, Q.J., Liu, X.M., Xu, J.M., Brookes, P.C., 2014. The identification of 'hotspots' of heavy metal pollution in soil–rice systems at a regional scale in eastern China. Sci. Total Environ. 472, 407–420.
Liu, X.M., Xu, J.M., Zhang, M.K., Huang, J.H., Shi, J.C., Yu, X.F., 2004. Application of geostatistics and GIS technique to characterize spatial variabilities of bioavailable micronutrient in paddy soils. Environ. Geol. 46 (2), 189–194.
Lu, A.X., Wang, J.H., Qin, X.Y., Wang, K.Y., Han, P., Zhang, S.Z., 2012. Multivariate and geostatistical analyses of the spatial distribution and origin of heavy metals in the agricultural soils in Shunyi, Beijing, China. Sci. Total Environ. 425, 66–74.
Lv, J., Liu, Y., Zhang, Z., Dai, J., 2013. Factorial kriging and stepwise regression approach to identify environmental factors influencing spatial multi-scale variability of heavy metals in soils. J. Hazard. Mater. 261, 387–397.
Matheron, G., 1963. Principles of geostatistics. Econ. Geol. 58 (8), 1246–1266.
Meklit, T., Van, M.M., Verstraete, S., Bonroy, J., Tack, F., 2009. Combining marginal and spatial outliers identification to optimize the mapping of the regional geochemical baseline concentration of soil heavy metals. Geoderma 148, 413–420.
Micó, C., Recatalá, L., Peris, M., Sánchez, J., 2006. Assessing heavy metal sources in agricultural soils of an European Mediterranean area by multivariate analysis. Chemosphere 65 (5), 863–872.
Mrvić, V., Kostić-Kravljanac, L., Čakmak, D., Sikirić, B., Brebanović, B., Perović, V., Nikoloski, M., 2011. Pedogeochemical mapping and background limit of trace elements in soils of Branicevo Province (Serbia). J. Geochem. Explor. 109, 18–25.
Nannoni, F., Protano, G., Riccobono, F., 2011. Fractionation and geochemical mobility of heavy elements in soil of a mining area in northern Kosovo. Geoderma 161, 63–73.
Otero, N., Tolosana-Delgado, R., Soler, A., Pawlowsky-Glahn, V., Canals, A., 2005. Relative vs. absolute statistical analysis of compositions: a comparative study of surface waters of a Mediterranean river. Water Res. 39 (7), 1404–1414.
Ottensen, R.T., Birke, M., Finne, T.E., Gosar, M., Locutura, J., Reimann, C., Tarvainen, T., 2013. Mercury in European agricultural and grazing land soils. Appl. Geochem. 33, 1–12.
Palumbo, B., Angelone, M., Bellanca, A., Dazzi, C., Hauser, S., Neri, R., Wilson, J., 2000. Influence of inheritance and pedogenesis on heavy metal distribution in soils of Sicily, Italy. Geoderma 95, 247–266.
Pawlowsky-Glahn, V., Buccianti, A., 2011. Compositional Data Analysis: Theory and Applications. John Wiley & Sons Canada, Limited, pp. 400.
Qishlaqi, Afshin, Moore, Farid, Forghani, Giti, 2009. Characterization of metal pollution in soils under two landuse patterns in the Angouran region, NW Iran; a study based on multivariate data analysis. J. Hazard. Mater. 172, 374–384.
Quinton, J.N., Catt, J.A., 2007. Enrichment of heavy metals in sediment resulting from soil erosion on agricultural fields. Environ. Sci. Technol. 41 (10), 3495–3500.
Reimann, C., Garrett, R.G., 2005. Geochemical background–concept and reality. Sci. Total Environ. 350 (1), 12–27.
Reimann, C., Kashulina, G., de Caritat, P., Niskavaara, H., 2001. Multi-element, multi-medium regional geochemistry in the European Arctic: element concentration, variation and correlation. Appl. Geochem. 16 (7), 759–780.
Reimann, C., Birke, M., Demetriades, A., Filzmoser, P., O'Connor, P. (Eds.), 2014. Chemistry of Europe's Agricultural Soils – Part A: Methodology and Interpretation of the GEMAS Data Set.
Rodríguez, J.A., Arias, M.L., Grau, J.M., 2006. Heavy metals contents in agricultural topsoils in the Ebro basin (Spain). Application of the multivariate geostatistical methods to study spatial variations. Environ. Pollut. 144 (3), 1001–1012.
Rodríguez, J.A., Nanos, N., Grau, J.M., Gil, L., López-Arias, M., 2008. Multiscale analysis of heavy metal contents in Spanish agricultural topsoils. Chemosphere 70, 1085–1096.
Rognerud, S., Hongve, D., Fjeld, E., Ottesen, R.T., 2000. Trace metal concentrations in lake and overbank sediments in southern Norway. Environ. Geol. 39 (7), 723–732.
Rousseeuw, P.J., Driessen, K.V., 1998. A fast algorithm for the minimum covariance determinant estimator. Technometrics 41, 212–223.
Saby, N.P.A., Thioulouse, J., Jolivet, C.C., Ratié, C., Boulonne, L., Bispo, A., Arrouays, D., 2009. Multivariate analysis of the spatial patterns of 8 trace elements using the French soil monitoring network data. Sci. Total Environ. 407 (21), 5644–5652.
Salminen, R., Gregorauskiene, G., 2000. Considerations regarding the definition of a geochemical baseline of elements in the surficial materials in areas differing in basic geology. Appl. Geochem. 15, 647–653.
Salminen, R., Batista, M.J., Bidovec, M., Demetriades, A., De Vivo, B., De Vos, W., Duris, M., Gilucis, A., Gregorauskiene, V., Halamić, J., Heitzmann, P., Lima, A., Jordan, G., Klaver, G., Klein, P., Lis, J., Locutura, J., Marsina, K., Mazreku, A., O'Connor, P.J., Olsson, S.A., Ottesen, R.-T., Petersell, V., Plant, J.A., Reeder, S., Salpeteur, I., Sandstrom, H., Siewers, U., Steenfelt, A., Tarvainen, T., 2005. FOREGS Geochemical Atlas of Europe, Part 1: Background Information, Methodology and Maps.
Sun, Y.B., Zhou, Q.X., Xie, X.K., Liu, R., 2010. Spatial, sources and risk assessment of heavy metal contamination of urban soils in typical regions of Shenyang, China. J. Hazard. Mater. 174 (1–3), 455–462.
Sutherland, R.A., 2000. Bed sediment-associated trace metals in an urban stream, Oahu, Hawaii. Environ. Geol. 39 (6), 611–627.
Tarvainen, T., Albanese, S., Birke, M., Ponavic, M., Reimann, The GEMAS Project Team, 2013. Arsenic in agricultural and grazing land soils of Europe. Appl. Geochem. 28, 2–10.
Wang, D., Shi, X., Wei, S., 2003. Accumulation and transformation of atmospheric mercury in soil. Sci. Total Environ. 304, 209–214.
Wang, D.F., Wei, Z.Y., Qi, Z.P., 2013. Background estimation of Cr in arable land soil of Hainan, China. China J. Trop. Crops 34 (1), 146–150 (With abstract in English).
Wedepohl, K.H., 1978. Handbook of Geochemistry. Vol. 2. Springer-Verlag, Berlin, Heidelberg, New York, pp. 1546.
Yuan, G.L., Sun, T.H., Han, P., Li, J., 2013. Environmental geochemical mapping and multivariate geostatistical analysis of heavy metals in topsoils of a closed steel smelter: capital iron & steel factory, Beijing, China. J. Geochem. Explor. 130, 15–21.
Yuan, G.L., Sun, T.H., Han, P., Li, J., 2014. Source identification and ecological risk assessment of heavy metals in topsoil using environmental geochemical mapping: typical urban renewal area in Beijing, China. J. Geochem. Explor. 136, 40–47.
Zhang, H.H., Li, F.B., Wu, Z.F., Li, D.Q., Xu, D.R., Yuan, H.X., 2008. Baseline concentrations and spatial distribution of trace metals in surface soils of Guangdong province, China. J. Environ. Qual. 37 (5), 1752–1760.
Zhao, K., Liu, X., Xu, J., Selim, H.M., 2010a. Heavy metal contaminations in a soil–rice system: identification of spatial dependence in relation to soil properties of paddy fields. J. Hazard. Mater. 181, 778–787.
Zhao, Y.C., Wang, Z.G., Sun, W.X., Huang, B., Shi, X.Z., Ji, J.F., 2010b. Spatial interrelations and multi-scale sources of soil heavy metal variability in a typical urban–rural transition area in Yangtze River Delta region of China. Geoderma 156, 216–227.